Nucleic Acids Research, 1993, Vol. 21, No. 1 **41–49**

Influence of tRNA tertiary structure and stability on aminoacylation by yeast aspartyl-tRNA synthetase

Joseph D.Puglisi+, Joern Pütz, Catherine Florentz and Richard Giegé*
UPR Structure des Macromolécules Biologiques et Mécanismes de Reconnaissance, Institut de Biologie Moléculaire et Cellulaire du CNRS, 15 rue René Descartes, F-67084 Strasbourg Cedex, France

Received October 26, 1992; Revised and Accepted December 4, 1992

ABSTRACT

Mutations have been designed that disrupt the tertiary structure of yeast $tRNA^{Asp}$. The effects of these mutations on both tRNA structure and specific aspartylation by yeast aspartyl-tRNA synthetase were assayed. Mutations that disrupt tertiary interactions involving the D-stem or D-loop result in destabilization of the base-pairing in the D-stem, as monitored by nuclease digestion and chemical modification studies. These mutations also decrease the specificity constant (k_{cat}/K_m) for aspartylation by aspartyl-tRNA synthetase up to 10^3-10^4 fold. The size of the T-loop also influences $tRNA^{Asp}$ structure and function; change of its T-loop to a tetraloop (-UUCG-) sequence results in a denatured D-stem and an almost 10^4 fold decrease of k_{cat}/K_m for aspartylation. The negative effects of these mutations on aspartylation activity are significantly alleviated by additional mutations that stabilize the D-stem. These results indicate that a critical role of tertiary structure in $tRNA^{Asp}$ for aspartylation is the maintenance of a base-paired D-stem.

INTRODUCTION

Specific aminoacylation of tRNAs by aminoacyl-tRNA synthetases (aaRSs) involves recognition of nucleotides presented in the proper orientation by the folded structure of the tRNA (1–4). The nucleotides important for specific aminoacylation by yeast aspartyl-tRNA synthetase (AspRS) have previously been determined (5); these are G_{34}, U_{35}, and C_{36} in the anticodon, G_{73} at the 3′-CCA terminus, and the $G_{10}\cdot U_{25}$ base pair in the D-stem (Fig. 1). Crystallographic analyses (3) and footprinting experiments (6) have demonstrated that these nucleotides are in regions of direct contact with the synthetase or in close proximity for $G_{10}\cdot U_{25}$ base pair. AspRS contacts the tRNA along the inner portion of the L-shaped tertiary structure and large portions of the tRNA are not in direct contact with protein.

The three-dimensional structure of $tRNA^{Asp}$ is well characterized (4, 7, 8), and involves an array of conserved and semi-conserved interactions mainly involving the D-stem of the tRNA (Fig. 1). The majority of nucleotides that participate in tertiary interactions are not in direct contact with AspRS in the crystal structure (3). Features of tRNA tertiary structure have been shown to be important in aminoacylation by certain aminoacyl-tRNA synthetases (e.g. yeast PheRS) (9, 10). However, other synthetases require only a simple subset of the tRNA structure for efficient recognition and aminoacylation. For example, *E.coli* AlaRS can aminoacylate an RNA helix that corresponds to the aminoacyl-acceptor stem of $tRNA^{Ala}$ (11).

To characterize the role of tertiary structure elements in the recognition and aminoacylation of yeast $tRNA^{Asp}$ by AspRS, we constructed a series of mutants that disrupt interactions responsible for the tRNA folding. Because the structures of both free $tRNA^{Asp}$ (7, 8) and $tRNA^{Asp}$ complexed with AspRS are known (3), the yeast $tRNA^{Asp}$/AspRS system represents an excellent model for understanding the role of tertiary interactions in stabilizing the folded structure of the tRNA and the contribution of tRNA tertiary structure features to recognition and aminoacylation by aminoacyl-tRNA synthetases. In the present study, the structure of mutant tRNAs were characterized, and their aminoacylation by AspRS determined by steady-state kinetics. The results indicate coupling among tertiary structure, secondary structure stability and tRNA aminoacylation, and point to a particular role of the D-stem in this process.

MATERIALS AND METHODS

Materials

Yeast AspRS (12) and T_7 RNA polymerase (13) were purified as described. Restriction enzyme BstN1 and T_4 polynucleotide kinase were from New England Biolabs (Beverly, MA, USA), bovine alkaline phosphatase was from Appligene (Strasbourg, France), nucleases S_1 and T_1 were from Pharmacia (St Quentin-en-Yvelines, France), diethylpyrocarbonate (DEPC) was from Aldrich (St Quentin Fallavier, France).

Preparation of tRNA transcripts

Plasmids that contain the genes for wild-type and mutant yeast $tRNA^{Asp}$ were prepared as described (5, 14). Plasmids were linearized with BstN1 and RNA molecules were transcribed using

* To whom correspondence should be addressed

+ Present address: Department of Chemistry, Massachusetts Institute of Technology, 77 Massachusetts Avenue, Cambridge MA 02139, USA

T_7 RNA polymerase. Transcriptions were performed in 40 mM Tris−HCl pH 8.1, 22 mM $MgCl_2$, 1 mM spermidine, 5 mM dithioerythritol, 0.01% Triton X-100, 4 mM each NTP and 5 mM GMP for 4 hours at 37°C. After phenol extraction and ethanol precipitation, transcripts were purified using denaturing polyacrylamide gel electrophoresis. Full length RNA was eluted from gel slices using a Schleicher & Schüll (Dassel, Germany) electroelution apparatus.

Aminoacylation of tRNA

Aspartylation of wild-type and mutant tRNA transcripts were performed in 0.1 M Hepes-KOH pH 7.5, 30 mM KCl, 10 mM $MgCl_2$, 5 mM ATP and 52 μM L-[^{3}H]aspartic acid at 30°C as described (15). These reactions were performed under steady-state conditions of enzyme and tRNA substrate concentrations (50nM to 10μM), and sub-saturating concentrations of aspartic acid (12). As a control, each group of mutants was tested in parallel with the $tRNA^{Asp}$ ($G_1 \cdot C_{72}$) transcript. Apparent K_m and k_{cat} values for aspartylation of tRNA transcripts were derived from Lineweaver−Burk plots.

Structure mapping of tRNA variants using enzymatic and chemical probes

tRNA transcripts were dephosphorylated using bovine alkaline phosphatase and 5′-end labeled using T_4 polynucleotide kinase. RNA was labeled at the 3′-end by first removal of the 3′-terminal nucleotides by digestion of 5 μg of tRNA with snake venom exonuclease. The 3′-CCA end was reconstituted by subsequent incubation with [α-^{32}P]CTP, ATP and (ATP, CTP):tRNA nucleotidyl-transferase as described (16).

Modification of tRNAs with DEPC (17) was performed using 3′-[^{32}P]-labeled transcripts. Modification reactions were carried out in 100 μl total volume of 50 mM Na cacodylate, pH 7.0 in the presence of 5 mM $MgCl_2$ (native conditions) or absence of $MgCl_2$ (semi-denaturing conditions). For each modification reaction, 20 μl of DEPC was added and modification reactions were carried out at 22°C, with occasional vortexing. Following DEPC modification, RNA was precipitated (20 min at −70°C) by addition of 5 μg unfractionated yeast tRNA, 15 μl of 3 M sodium acetate (pH 4.6) and 300 μl of ethanol. The RNA pellet was resuspended in 100 μl of 0.3 M sodium acetate and reprecipitated by addition of 300 μl ethanol. Strand scission was induced by dissolving the RNA pellet in 20 μl of aniline:acetic acid (pH 5.0) and incubating for 20 min at 60°C. Samples were then dried and dissolved in 20 μl of H_2O; this was repeated twice to insure complete removal of the aniline. The final pellet was resuspended in 10 μl of 8 M urea. Cleavage reactions were analyzed by denaturing polyacrylamide (15%) gel electrophoresis and autoradiography.

Structure mapping and footprinting with nucleases S_1 and T_1 were performed with 5′-[^{32}P]-labeled transcripts in 10 μl of 5 mM $MgCl_2$, 50 mM NaCl, 10 mM 2-(N-morphilino)-ethane sulfonic acid, pH 6.5. Labeled and unlabeled transcript were mixed to give a total transcript concentration of 1 μM in 10 μl reaction volume. For footprinting experiments, yeast AspRS was dialyzed against 10 mM $MgCl_2$, 50 mM NaCl, 10 mM 2-(N-morphilino)-ethane sulfonic acid, pH 6.5 in a Centricon 30 (Amicon, Beverly, MA, USA). AspRS was added to footprinting reactions to give a total concentration of 4 μM. This assures saturation of tRNAs with wild-type dissociation constants (*ca.* 100nM) and allows qualitative comparison of relative binding affinities of tRNA variants. Digestions were performed at 22°C for 3 min using 1 unit of S_1 or 0.001 units of nuclease T_1. Reactions were stopped by addition of 40 μl of 0.4 M sodium acetate, phenol extraction, and ethanol precipitation.

Ultraviolet absorbance melting experiments

UV absorbance melting curves (18) were obtained on a Beckmann UV-Vis spectrometer equipped with a temperature controller. Absorbance was monitored at 260 nm and temperature was increased at 0.5°C/min. Melting curves were obtained at transcript concentrations of 1−2 μM in 5 mM $MgCl_2$, 50 mM NaCl, 10 mM Na cacodylate, pH 7.0.

RESULTS

A series of mutations (shown in Fig. 2) were constructed with changes in two regions of $tRNA^{Asp}$ involved in tertiary interactions, the D-stem and loop and the T-loop;the interdigitation between these two loops contribute to the L-shape of the tRNA. Steady-state kinetic parameters for aspartylation of all mutants are shown in Table 1. The preponderant effect of most of these mutations is on the K_m for aspartylation, in contrast to the k_{cat} effects observed for most mutations of the identity elements (5).

D-stem mutations

As shown previously, conservative mutations at base pair $G_{10} \cdot U_{25}$, a position known to be important for $tRNA^{Asp}$ recognition, result in loss of aminoacylation efficiency (5). Mutation of G_{10}, conserved in all tRNAs, to A_{10} had a strongly negative effect on aspartylation (30-fold decrease in k_{cat}/K_m). Conversion of U_{25} to C_{25} resulted in a decrease of k_{cat}/K_m of 8 fold. Conversion of the $U_{11} \cdot A_{24}$ base-pair to either $C_{11} \cdot A_{24}$ or $U_{11} \cdot G_{24}$ had a strongly deleterious effect on aspartylation activity; the kinetic specificity constant (k_{cat}/K_m) decreased

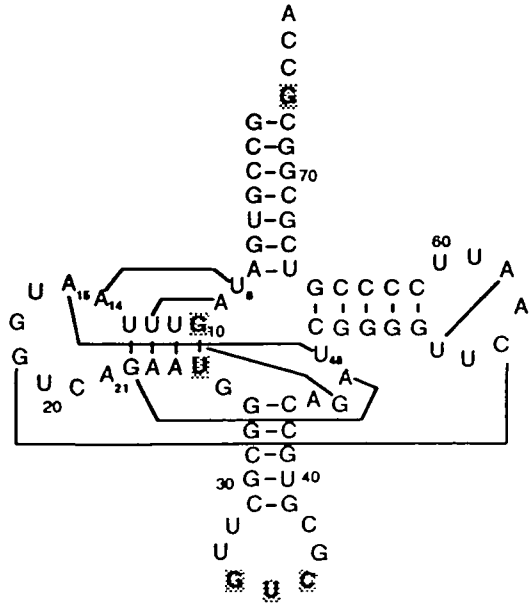

Figure 1. Sequence of yeast $tRNA^{Asp}$ transcript, showing critical tertiary interactions; the $U_1 \cdot A_{72}$ base pair has been changed to $G_1 \cdot C_{72}$ with no effect on aspartylation. The nucleotide determinants for specific aspartylation by yeast AspRS are shaded.

56–140 fold compared to wild-type transcript. Upon double mutation to Watson–Crick base pairing ($U_{11}\cdot A_{24}$ changed to $C_{11}\cdot G_{24}$), aspartylation activity was restored to near wild-type level. $U_{11}\cdot A_{24}$ is the only base pair from the D-stem that is not involved in base-triple formation (Fig. 1). Change of the $U_{12}\cdot A_{23}$ pair to $C_{12}\cdot G_{23}$ was made with the additional change of A_9 to G_9; G_9 is only observed in tRNA sequences when a $C_{12}.G_{23}$ pair is present, although the exact geometry of this pair is not obvious (4). The mutation of these three nucleotides in $tRNA^{Asp}$ had little effect on aspartylation. The last base pair of the D-stem, $U_{13}\cdot G_{22}$, was replaced by $C_{13}.G_{22}$. This change had no effect on aminoacylation.

The structures of several of these D-stem mutants were probed in solution using DEPC reactivity at the N7 position of adenines (Fig. 3A). DEPC is useful since the solvent accessibilities of individual adenines can be probed in the presence and absence of Mg^{2+} (19). For both modified $tRNA^{Asp}$ (17) and wild-type transcript (14), only A_{21} is significantly reactive in the presence of 5 mM Mg^{2+} (see also Fig. 3B). All other adenines in the D-stem and loop (A_{14}, A_{15}, A_{23}, A_{24}) as well as A_9 and A_{44} are reactive only in the absence of Mg^{2+} (semi-denaturing conditions). Several mutant transcripts show modification patterns in the presence of 5 mM Mg^{2+} that are different from that of wild-type transcript. For the $U_{11}\cdot A_{24}$ to $U_{11}\cdot G_{24}$ mutant, all D-stem and loop adenines are as accessible in 5 mM Mg^{2+} as in the absence of Mg^{2+}, especially A_{23} located in middle of the stem. This suggests an opening of the stem. The $G_{10}\cdot U_{25} \rightarrow A_{10}\cdot U_{25}$ mutant transcript showed a slightly increased reactivity in 5 mM Mg^{2+} compared to wild-type transcript. Only the mutant in which $U_{11}.A_{24}$ was changed to $C_{11}\cdot G_{24}$ had a DEPC modification pattern that was similar to wild-type transcript in 5 mM Mg^{2+}. The modification of D-stem and loop adenines, except for A_{21}, was weak.

D-loop mutations

The D-loop of $tRNA^{Asp}$ is involved in tertiary interactions that stabilize its folded structure. Nucleotide A_{21} is highly conserved among tRNA sequences, but is not directly involved in a tertiary

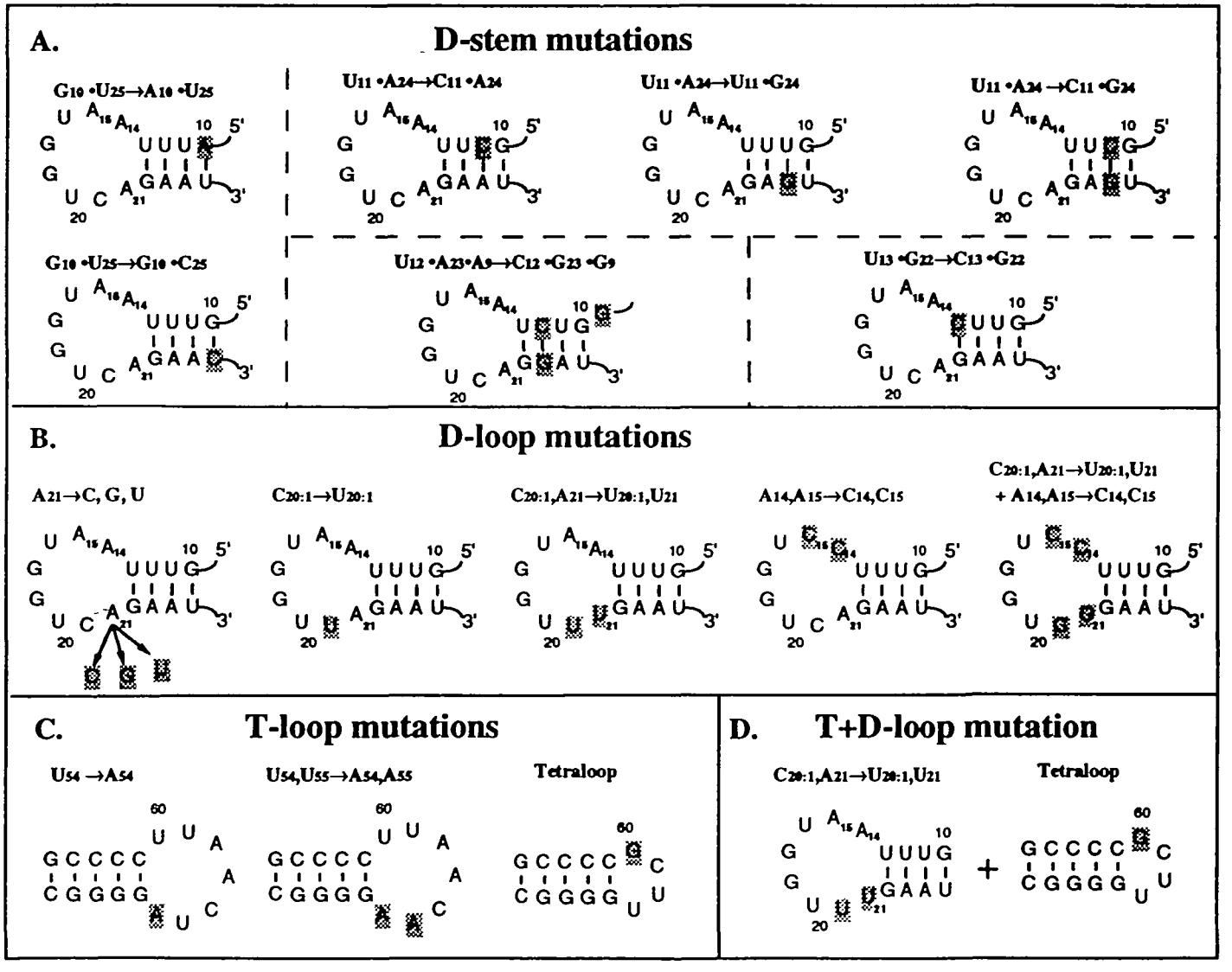

Figure 2. tRNA variants characterized. Only the region of the mutation is shown; mutated positions are highlighted. In the tetraloop mutant, residue G_{60} replaces the wild-type sequence $A_{57}AUU_{60}$.

Table 1. Kinetic parameters for aspartylation of yeast $tRNA^{Asp}$ variant transcripts with yeast AspRS.

Mutant type	$tRNA^{Asp}$ variant	K_m(nM)	$k_{cat}(s^{-1})$	k_{cat}/K_m (relative)	loss of efficiency (x-fold)
tRNAAsp	$(U_1 \cdot A_{72}) \rightarrow (G_1 \cdot C_{72})$	50	0.52	1	1
D-stem	$G_{10} \cdot U_{25} \rightarrow A_{10} \cdot U_{25}$	1400	0.44	0.030	33*
	$G_{10} \cdot U_{25} \rightarrow G_{10} \cdot C_{25}$	240	0.31	0.12	8*
	$U_{11} \cdot A_{24} \rightarrow C_{11} \cdot A_{24}$	4500	0.33	7.1×10^{-3}	140
	$U_{11} \cdot A_{24} \rightarrow U_{11} \cdot G_{24}$	20000	3.7	0.018	56
	$U_{11} \cdot A_{24} \rightarrow C_{11} \cdot G_{24}$	100	0.38	0.37	3
	$\{(U_{12} \cdot A_{23})\text{-}A_9\} \rightarrow \{(C_{12} \cdot G_{23})\text{-}G_9\}$	150	0.54	0.35	3
	$U_{13} \cdot G_{22} \rightarrow C_{13}\text{-}G_{22}$	50	0.32	0.62	2
D-loop	$A_{21} \rightarrow C_{21}$	130	0.54	0.40	3
	$A_{21} \rightarrow G_{21}$	270	0.30	0.11	9
	$A_{21} \rightarrow U_{21}$	150	0.34	0.23	5
	$C_{20.1} \rightarrow U_{20.1}$	40	0.38	0.91	1
	$C_{20.1}, A_{21} \rightarrow U_{20.1}, U_{21}$	45	0.35	0.75	1.3
	$A_{14}, A_{15} \rightarrow C_{14}, C_{15}$	1800	0.029	1.5×10^{-3}	650
	$A_{14}, A_{15}, C_{20.1}, A_{21} \rightarrow C_{14}, C_{15}, G_{20.1}, G_{21}$	100	0.13	0.13	8
T-loop	$U_{54} \rightarrow A_{54}$	100	0.50	0.48	2.1
	$U_{54}, U_{55} \rightarrow A_{54}, A_{55}$	120	0.40	0.32	3
	$\text{-}U_{54}UCAAUU_{60}\text{-} \rightarrow \text{-}U_{54}UCG_{60}\text{-}$	8400	0.010	1.1×10^{-4}	87000
T- and D-loops	$\text{-}U_{54}UCAAUU_{60}$, $C_{20.1}$, $A_{21} \rightarrow \text{-}U_{54}UCG\text{-}$, $U_{20.1}, U_{21}$	21000	0.72	0.033	30

All variants were constructed from the $G_1 \cdot C_{72}$ mutant, which shows equivalent aspartylation parameters to those of fully modified $tRNA^{Asp}$ and $U_1 \cdot A_{72}$ transcripts. Apparent K_m and k_{cat} values for each $tRNA^{Asp}$ variant, obtained at sub-saturating concentrations of amino acid, were derived from a Lineweaver–Burk plot as described in 'Materials & Methods'. k_{cat}/K_m values for replicate experiments varied at most 15%. The $U_{11} \cdot G_{24}$ mutant had an anomalously high K_m and the corresponding values or k_{cat} and K_m are less precise.

* see ref. (5).

interaction (8); this position was mutated to the three other possible nucleotides (Fig. 2B) and the activity (Table 1) and structure (Fig. 3B) of the mutants were tested. Mutation to C_{21} had little effect on aspartylation activity: k_{cat}/K_m for aspartylation was decreased only 3-fold from the wild-type value. Chemical mapping experiments showed little disruption of structure for this mutant (Fig. 3B) as compared to wild-type. Mutation to U_{21} produced only a slightly stronger effect on aspartylation : k_{cat}/K_m was only reduced 5-fold. Mutation to G_{21} produced the strongest effect on aspartylation activity—k_{cat}/K_m was reduced 9-fold. Chemical mapping experiments with DEPC showed that adenines in the D-stem of both mutants were highly reactive in 5 mM Mg^{2+}. Mutation of position $C_{20.1}$ to $U_{20.1}$ had no effect on structure or activity.

Several mutants were designed to affect tertiary pairs involving the D-loop. A double mutant, in which both $C_{20.1}$ and A_{21} were changed to $U_{20.1}$ and U_{21}, gave aminoacylation kinetics similar to those of wild-type transcript. These mutations allow possible Watson–Crick base pairing with A_{14} and A_{15}, which would compete with the tertiary interactions involving these nucleotides. A_{14} and A_{15} were strongly modified by DEPC in 5 mM Mg^{2+} (Fig. 3B); thus this mutant has a perturbed tertiary structure but is aminoacylated like wild-type. Mutation of both A_{14} and A_{15} to C_{14} and C_{15} destroys conserved tertiary interactions with these positions (Fig. 2B). This double mutation had a strongly deleterious effect on aspartylation activity—k_{cat}/K_m was decreased 650-fold from the wild-type value. Structure mapping experiments of this mutant using single-strand specific nucleases S_1 and T_1 (Fig. 4A) showed that the D-stem between U_{25} and A_{21} is accessible to these probes; these regions are only weakly accessible in wild-type $tRNA^{Asp}$.

UV absorbance melting curves were performed to assess the effect of certain mutations in the D-loop on overall structural stability. In 50 mM Na cacodylate buffer, wild-type and mutant transcripts exhibited similar broad transitions (data not shown). On addition of 5 mM Mg^{2+}, the melting curve for the wild-type transcript changed drastically and showed a cooperative transition at 65°C. Similar behavior was observed for the $C_{20.1} \rightarrow U_{20.1}$ mutant. The $A_{21} \rightarrow C_{21}$ mutant had a similar melting curve with a transition at lower temperature (~55°C). For other mutants- $A_{21} \rightarrow G_{21}$, $A_{21} \rightarrow U_{21}$ and the two double mutants of the D-loop- addition of 5 mM Mg^{2+} had little effect on the melting behavior and the melting curves were broad and non-cooperative as in the absence of Mg^{2+} (Fig. 5).

T-loop mutation

To understand the interaction between the T- and D-loop, mutants were constructed that altered the sequence or size of the T-loop of $tRNA^{Asp}$ (Fig. 2C). The conserved nucleotide U_{54} was first changed to A_{54}, and in a second mutant it was changed together with U_{55} to A_{54} and A_{55}, which permits base pairing between positions 54 and 59, and between positions 54/55 and 59/60. These mutants were aspartylated only 2- to 3-fold worse than wild-type transcript. In the double mutant, DEPC modified A_{57} and A_{58} within the altered T-loop in 5 mM Mg^{2+}, whereas A_{54} and A_{55} were virtually unreactive (Fig. 3B). In the wild-type

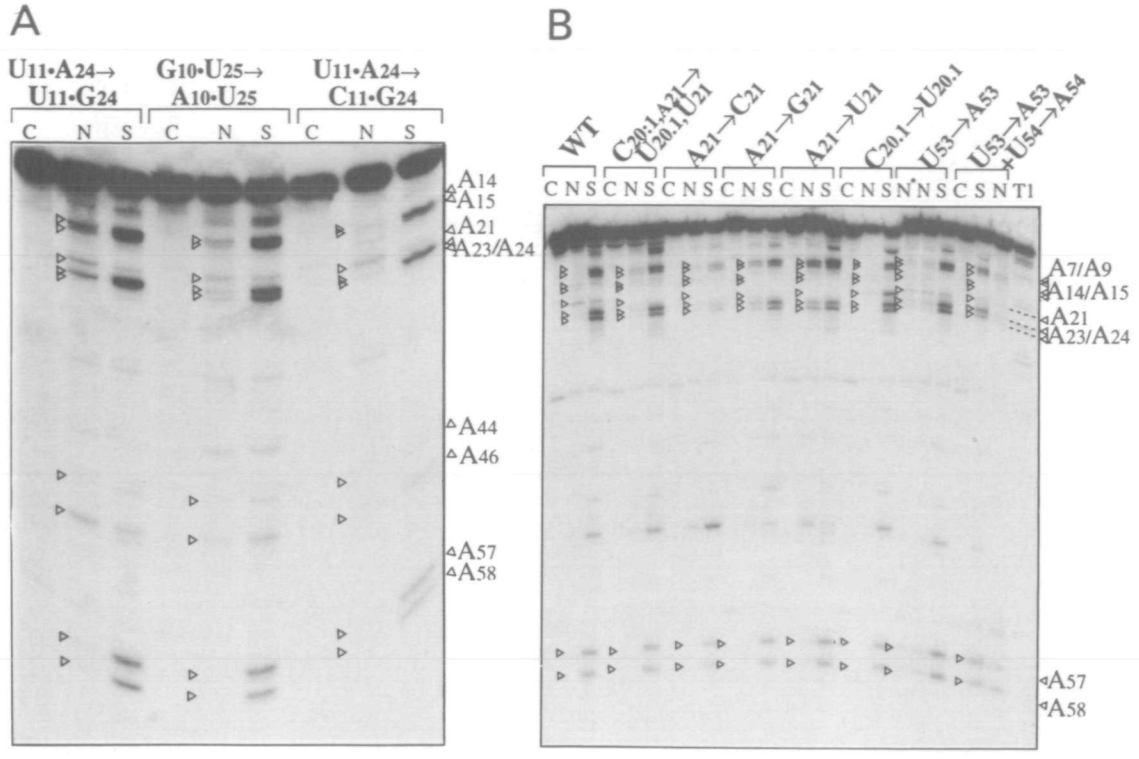

Figure 3. Autoradiographs showing DEPC modification of $tRNA^{Asp}$ transcripts containing mutations in the D-stem (**A**) or in the D-loop and T-loop (**B**). Modifications were performed under native (N) conditions (5 mM $MgCl_2$, 50 mM Na cacodylate, pH 7.0) or semi-denaturing (S) conditions (50 mM Na cacodylate, pH 7.0) at 22°C. No DEPC was added to the control lanes (C). Triangles mark positions discussed in the text. In (A), the $C_{11}\cdot G_{24}$ mutant gives a modification pattern similar to that for wild-type transcript.

transcript, A_{57} and A_{58}, which are involved in T-loop folding, were only modified in the absence of Mg^{2+}. These results indicate an alteration of T-loop structure upon mutation, probably a reduction in loop size to 3 nucleotides.

A mutant $tRNA^{Asp}$ with a T-loop consisting of a stable tetraloop sequence -UUCG- (20) (Fig. 2C) was very poorly aspartylated—k_{cat}/K_m was reduced 8700-fold. The D-stem of this mutant was strongly accessible to nucleases S_1 and T_1 (Fig. 4B). Likewise, all adenines in the D-stem of this mutant were highly accessible in 5 mM Mg^{2+} (data not shown).

Compensatory D- and T-loop mutations

The D-stem in $tRNA^{Asp}$ is thermodynamically unstable in the absence of tertiary structure (21). This instability may explain the deleterious effect of certain mutations on aspartylation. We attempted to compensate the negative effect on aspartylation of both the $A_{14},A_{15} \rightarrow C_{14},C_{15}$ mutant and the T-loop shortening to -UUCG- mutation by stabilizing the D-stem (Fig. 6). For the $A_{14},A_{15} \rightarrow C_{14},C_{15}$ mutant, $C_{20.1}$ and A_{21} were changed to $G_{20.1},G_{21}$ to allow the extension of the D-stem by two G.C base pairs. For the shortened T-loop mutant (-UUCG- tetraloop), $C_{20.1},A_{21}$ were changed to $U_{20.1},U_{21}$ to allow the extension of the D-stem by two A.U pairs.

Both mutants gave significantly improved aspartylation (Table 1). For the $C_{14},C_{15} + G_{20.1},G_{21}$ mutant, aspartylation specificity improves 81-fold upon stabilization of the D-stem; k_{cat}/K_m was reduced only 8-fold from the wild-type value, which results mostly from a decrease in k_{cat}. For the T-loop mutant (-UUCG- tetraloop + $C_{20.1},A_{21} \rightarrow U_{20.1},U_{21}$), k_{cat}/K_m was improved 290-fold over the non-stabilized D-stem. Also, k_{cat}/K_m was reduced 30-fold relative to wild-type $tRNA^{Asp}$, although k_{cat} equals the wild-type value.

The structures of these mutant transcripts were compared by S_1 and T_1 nuclease cleavage. As discussed above, the $A_{14},A_{15} \rightarrow C_{14},C_{15}$ mutant has a D-stem that is strongly accessible to single-stranded probes. Upon addition of two possible G.C pairs ($C_{14},C_{15} + G_{20.1},G_{21}$), the D-stem is much less accessible to S_1 and T_1 cleavage (Fig. 4A), consistent with stabilization of the stem. Strong cuts were only observed at G_{18}, G_{19}, U_{20}, in the potential 4-membered loop.

Specifically bound AspRS protects the anticodon loop from cleavage by single-strand specific probes (22). Nuclease digestions were performed in the presence of 4 μM AspRS, which is sufficient concentration to saturate the wild-type transcript. In the presence of AspRS, the anticodon loop of the $A_{14},A_{15} \rightarrow C_{14},C_{15}$ mutant is weakly protected from both S_1 and T_1 cleavage (around nucleotide G_{34}); the intensity of cleavage in the D-stem is also reduced. In contrast, the anticodon loop for the A_{14}, $A_{15} \rightarrow C_{14},C_{15} + C_{20:1},A_{21} \rightarrow G_{20.1},G_{21}$ mutant is strongly protected from nuclease cleavage by AspRS. Enzyme cleavage in the 4-membered D-loop was also reduced. These results show that the C_{14},C_{15} mutant interacts weakly, whereas the double mutant A_{14}, $A_{15} \rightarrow C_{14},C_{15} + C_{20:1},A_{21} \rightarrow G_{20.1},G_{21}$ interacts strongly with AspRS. This is consistent with the relative K_m values for the two mutants (Table 1).

Similar experiments were performed for the T-loop mutants (with -UUCG- tetraloops). Both the T-loop → -UUCG- and T-loop → -UUCG- + $C_{20:1},A_{21} \rightarrow G_{20.1},G_{21}$ mutants had similar

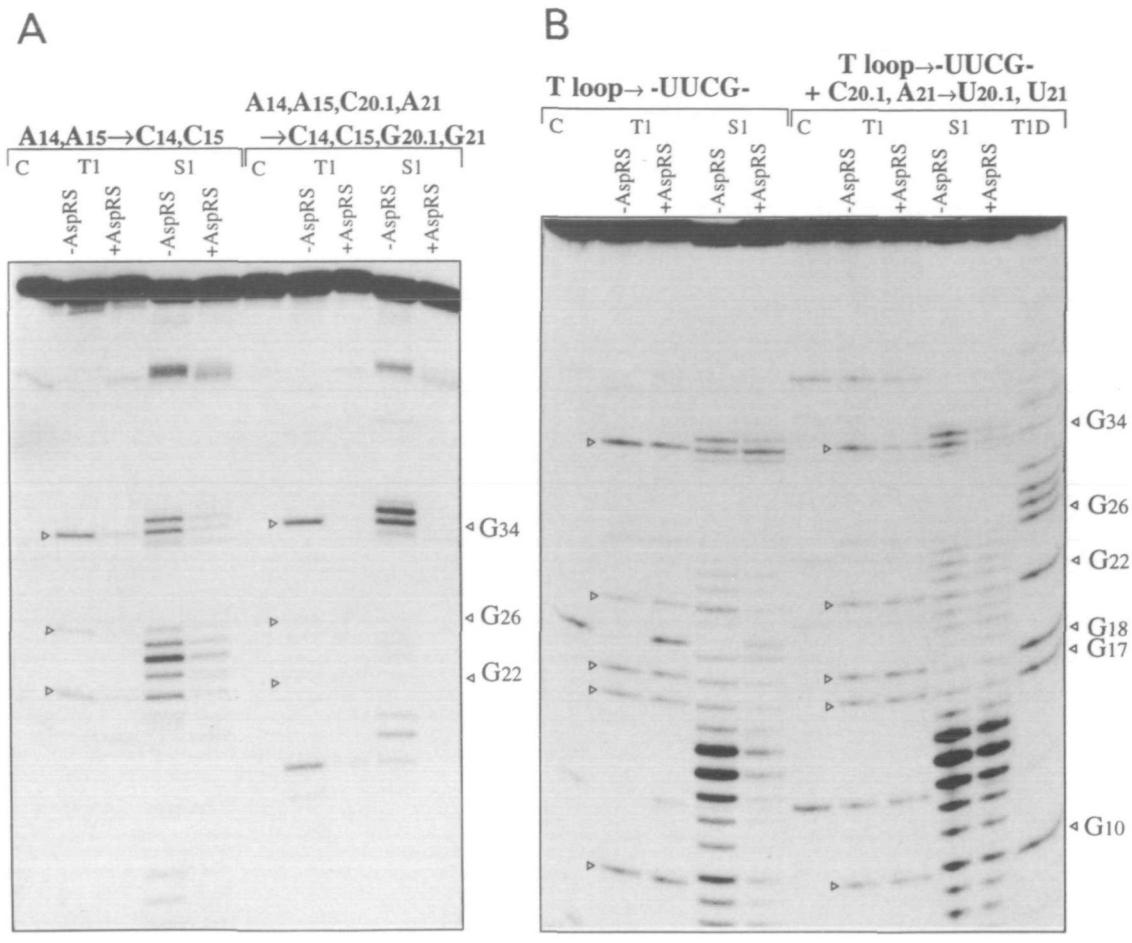

Figure 4. Autoradiographs showing enzymatic digestion of $tRNA^{Asp}$ variants in which tertiary interactions to the D-loop were disrupted **(A)** and in which tertiary interactions between the D-loop and T-loop were disrupted **(B)**. Digestions with nuclease S_1 (S1) or ribonuclease T_1 (T1) were performed in the absence (−AspRS) or presence (+ AspRS) of 4μM yeast AspRS. Control lanes **(C)** contained AspRS and RNA, but no added nuclease. In (B), a digestion was performed with nuclease T_1 under denaturing conditions (T_1D). Conditions are fully described in the section 'Materials and Methods'.

S_1 and T_1 digestion patterns (Fig. 4B). The D-stem and loop was highly accessible to cleavage; strongest cleavage was observed between U_{12} and A_{15}. Upon addition of 4 μM AspRS, no protection from cleavage of the anticodon is observed for the -UUCG- tetraloop mutant. Cleavage of the D-stem is somewhat reduced. Some protection of the anticodon is observed for the -UUCG- + $U_{20.1}$,U_{21} mutant, whereas no protection of the D-stem is observed. The weak interaction of both mutants with AspRS is consistent with their relative K_m values.

DISCUSSION

A defining feature of tRNAs is the conserved set of tertiary interactions. A number of studies have demonstrated that D-stem stability is tightly coupled to the presence of tertiary interactions (21, 23). The isolated D-stem consists of 2 A·U and 2 G·U base pairs. In 500 mM NaCl and no Mg^{2+}, the D-stem and tertiary interactions of yeast $tRNA^{Asp}$ melt together at 51°C, whereas the D-stem does not even form in an isolated half-molecule of $tRNA^{Asp}$ (21). The interdependence of D-stem and tertiary structure stability is not surprising since three triple interactions plus three tertiary pairs are formed between nucleotides of the

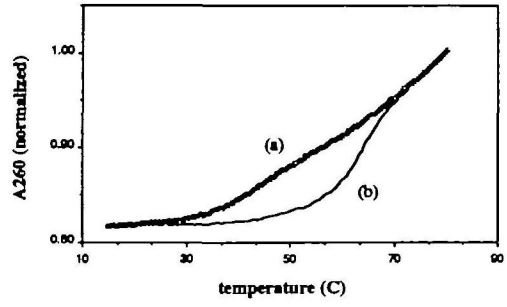

Figure 5. UV absorbance melting curves of wild-type and mutant ($C_{20.1}$,A_{21} → $U_{20.1}$,U_{21}) $tRNA^{Asp}$ transcripts in the absence (a) and presence (b) of 5 mM $MgCl_2$. Buffer conditions were 50 mM Na cacodylate, pH 7.0. Absorbance was monitored at 260 nm, and normalized for differences in tRNA concentrations.

D-stem and loop and nucleotides elsewhere in the tRNA (see Fig. 1). In this study, mutations that were designed to disrupt tertiary interactions in $tRNA^{Asp}$ also led to disruption of the D-stem, as observed by nuclease and chemical mapping experiments.

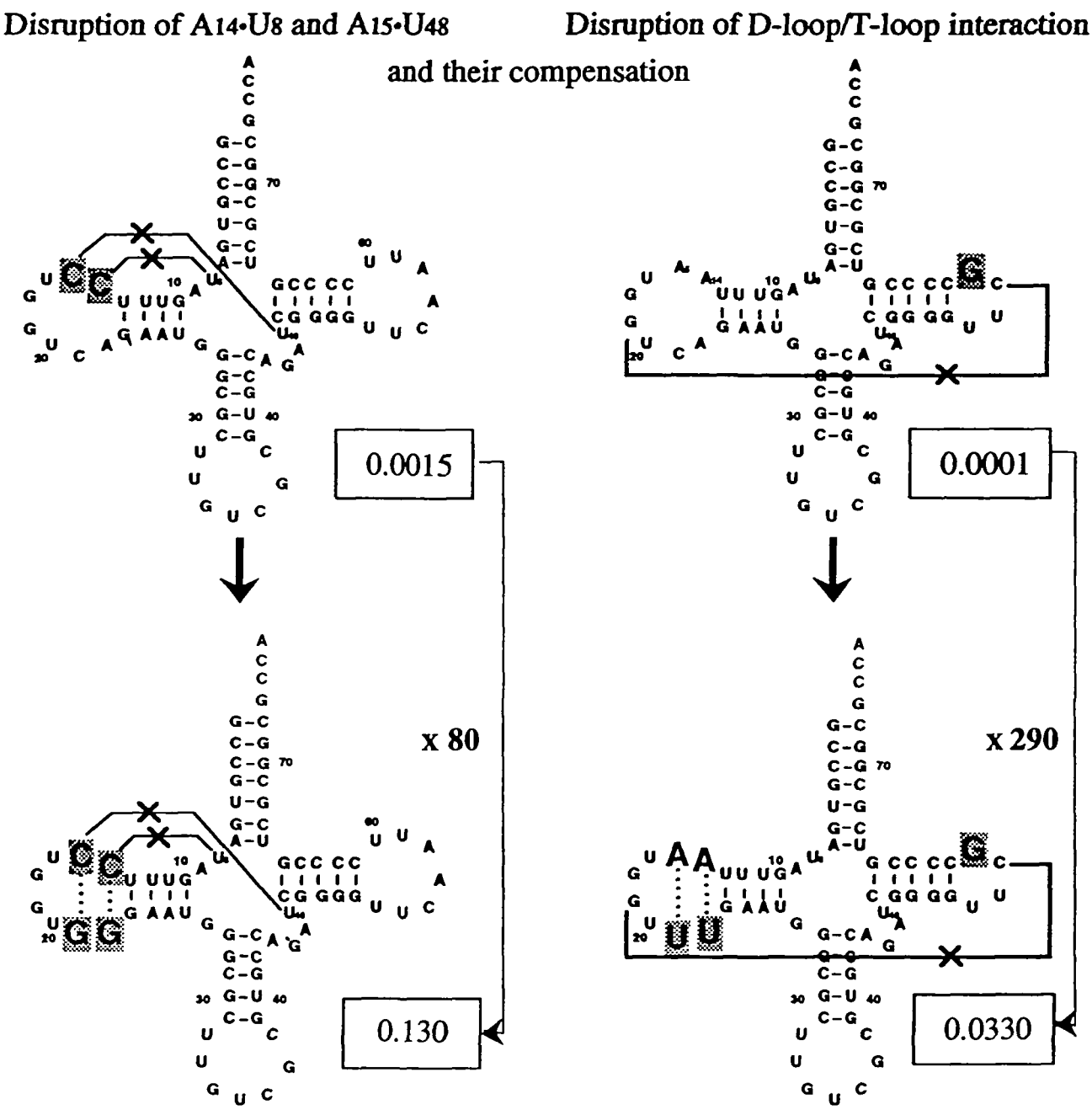

Figure 6. Disruption of tertiary interaction in $tRNA^{Asp}$ and their compensation. Stabilization of the D-stem of $tRNA^{Asp}$ compensates the deleterious effects of tertiary structure mutations. Mutated nucleotides and disrupted tertiary interactions are indicated. k_{cat}/K_m values relative to wild-type $tRNA^{Asp}$ (boxed) and their improvement upon stabilization of the D-stem (in bold) are shown. The two compensatory base pairs that extend the D-stem are indicated.

Mutation of nucleotides A_{14} and A_{15} in the D-loop, which are involved in tertiary interactions with U_8 and U_{48}, both resulted in denatured D-stems. Interestingly, mutation of conserved nucleotide A_{21} also led to disruption of the structure. This nucleotide is not directly involved in tertiary interactions, but is involved in stacking and steric contacts with A_{14}. Mutation to C_{21} had the smallest effect on tRNA structure and stability, whereas mutation to G_{21} had the largest effect. These results correlate with possible poor steric contacts with A_{14} upon mutation to G_{21}. More drastic mutations considerably affected the tRNA structure. Mutation of A_{14} and A_{15} to C_{14} and C_{15} disrupts two conserved tertiary pairs, $A_{14}\cdot U_8$ and $A_{15}\cdot U4_8$. Indeed, the D-stem of this mutant was highly accessible to single-strand probes and nucleases under native conditions.

Relatively large hairpin loops (7–9 nucleotides) are a conserved feature among tRNAs (4); this contrasts with the preference for smaller loops (3–5 nucleotides) in ribosomal RNAs (24). The larger loops in tRNA may be better suited to interact with other regions of tRNA or other RNAs than smaller loops. The T-loop of $tRNA^{Asp}$ interacts with the D-loop,

although in one crystal structure, the $G_{18}\cdot C_{56}$ tertiary pair is disrupted (8, 25). In the present study, both subtle and more drastic changes were introduced in the T-loop of $tRNA^{Asp}$. Mutation of the conserved U_{54},U_{55} residues to A_{54},A_{55} changes the structure of the T-loop, since these nucleotides can base pair with U_{59},U_{60}. More drastic changes of the T-loop of $tRNA^{Asp}$, which normally has the sequence (-U_{54}UCAAUU_{60}-) to a tetraloop sequence (-UUCG-) disrupted both the tertiary structure and D-stem as shown by chemical and enzymatic probes. Thus, the stable, compact tetraloop structure (26) is not compatible with tRNA tertiary structure.

Specific binding of Mg^{2+} stabilizes the folded tertiary structure of tRNAs. Crystallographic analyses have shown that at least three Mg^{2+} ions are bound specifically to $tRNA^{Phe}$ (27, 28) and $tRNA^{Asp}$ (29) in the region of the D-stem . These ions stabilize unfavorable electrostatic interactions within the tertiary structure. Addition of 10 mM Mg^{2+} shifts the UV melting curve of the wild-type transcript by 20°C, consistent with this stabilization. Adenines that are accessible to DEPC in the absence of Mg^{2+} are protected on addition of the ion. Magnesium ions did not stabilize the tertiary structure of many of the mutants in this study, as shown by both chemical modification and UV melting experiments. The G_{21} and U_{21} mutants gave altered UV melting curves in 5 mM $MgCl_2$; the broad transitions observed ($T_m \sim 55°C$) for these mutants contrast with the much sharper transition observed for the wild-type (and C_{21}) sequences ($T_m = 65°C$). These broad melting curves were unchanged upon addition or removal of Mg^{2+}. Thus, the effect of the D-stem, D-loop and T-loop mutations are similar: there is a cooperative loss of tertiary structure and D-stem stability coupled with a loss of Mg^{2+} binding. The loss of thermodynamic stability of these tertiary mutants is probably coupled with the loss of specific Mg^{2+} binding sites (30).

The mutations of the D-loop or T-loop do not involve nucleotides in direct contact with AspRS. These mutations affect aspartylation by disrupting the tertiary and secondary structure of $tRNA^{Asp}$. Mutational studies have shown that $G_{10}\cdot U_{25}$ in the D-stem is a determinant for specific aspartylation (5). Recognition of this base pair requires an intact D-stem. Since tertiary structure formation and D-stem stability are coupled in $tRNA^{Asp}$, mutations that affect either resulted in decreased aspartylation. Mutations that disrupt base pairing in the D-stem significantly decreased k_{cat}/K_m for aspartylation by 60−140-fold. Aspartylation activity was restored by introduction of other Watson-Crick base pairs at positions 11.24. The aspartylation kinetics of most tertiary structure mutants were reduced by factors of 10 to 10^4.

The effect of these mutations involves a major contribution from the loss of a base-paired D-stem. The deleterious effects of these mutations were compensated by further mutations that stabilized the base pairing in the D-stem. k_{cat}/K_m for the C_{14},C_{15} mutant was improved by 80-fold by mutating $C_{20.1}$ and A_{21} to $G_{20.1}$ and G_{21} to extend the D-stem by two additional base pairs. Likewise, k_{cat}/K_m for the T-loop mutant (-UUCG-) was improved by 290-fold by extending the D-stem by two A.U base pairs. Although mutants with stabilized D-stems are good substrates for AspRS, they do not contain the canonical set of tertiary interactions, and probably do not adopt a stable L-shaped tertiary structure in solution. Thus, the precise tertiary structure of tRNA does not seem to be an absolute requirement for aspartylation by AspRS.

Different aminoacyl-tRNA synthetases recognize tRNAs in different ways (1, 3, 4). Previous studies of tertiary structure mutants of $tRNA^{Phe}$ have shown that yeast PheRS is sensitive to tRNA tertiary structure (9, 10). Mutations that destabilized conserved tertiary interactions reduced k_{cat}/K_m values for phenylalanation by only 10-fold at most, in contrast to the more drastic effects of mutation on aspartylation observed in this study. Disruption of tertiary interactions in yeast $tRNA^{Phe}$ probably does not lead to a cooperative unfolding of the D-stem, since this stem is quite stable (3 G.C pairs and 1 A.U pair). Thus, mutations of tertiary structure have more global effect on $tRNA^{Asp}$ structure. Experiments in which yeast $tRNA^{Phe}$ identity determinants were transplanted into a $tRNA^{Asp}$ structural framework and yeast $tRNA^{Asp}$ identity nucleotides were transplanted into a $tRNA^{Phe}$ structural context have shown that yeast PheRS has stricter requirements for precise tertiary structure in the region of the D-loop than yeast AspRS (10). This is consistent with the results presented here, where AspRS has a strong requirement for a base-paired D-stem and is less sensitive to the overall tertiary structure.

The crystal structure of yeast $tRNA^{Asp}$ with AspRS has shown that contacts are made with the anticodon loop and stem, the base of the D-stem and the 3′ region of the acceptor stem (3). This recognition mode is probably not as dependent on the overall tertiary structure of the tRNA than, for example, that of *E.coli* GlnRS, which has a large interaction surface with $tRNA^{Gln}$ (1).

There are many examples of naturally occurring tRNA-like molecules that differ in tertiary structure from canonical tRNA. Mitochondrial tRNAs often lack conserved nucleotides, or even entire stem-loops, that are involved in tertiary interactions in cytoplasmic tRNAs (31, 32). Intriguingly, certain mitochondrial synthetases (e.g. bovine mitochondrial PheRS) efficiently aminoacylate both their cognate mitochondrial tRNAs and cytoplasmic analogs, whereas the cytoplasmic synthetase did not efficiently aminoacylate the mitochondrial tRNA (33). Thus, mitochondrial synthetases, which normally recognize tRNA substrates with relaxed tertiary structures, may be less sensitive to tRNA tertiary structure than their cytoplasmic analogs. Certain synthetases are involved in aminoacylation of tRNA-like structures found at the 3′-ends of some plant viral RNAs (e.g. HisRS, TyrRS, and ValRS) (4, 34), whereas other synthetases bind cellular tRNA-like structures (35, 36). Although these may resemble tRNAs, their precise tertiary structures are different. The synthetases that recognize these structures may have more relaxed requirements for precise tRNA tertiary structure.

In summary, mutations that disrupt conserved tertiary interactions in yeast $tRNA^{Asp}$ have a cooperative effect on the folding of this molecule. For this reason, specific aspartylation of these mutants is significantly reduced. If cooperative unfolding of $tRNA^{Asp}$ is blocked by stabilization of the D-stem, aspartylation is efficient, even in the absence of certain conserved tertiary interactions. Further characterization of RNA folding and stability as well as structural studies on tRNA-synthetase complexes will allow us to understand in detail the role of RNA tertiary structure (37) in protein recognition.

ACKNOWLEDGMENTS

This work was supported by grants from the Centre National de la Recherche Scientifique (CNRS), Ministère de la Recherche et de la Technologie (MRT), Université Louis Pasteur

(Strasbourg), and by an award from the Human Frontier Science Program. JDP was the recipient of an EMBO long-term fellowship. JP was partially supported by the Human Frontier Science Program.

REFERENCES

1. Rould,M.A., Perona,J.J., Söll,D. and Steitz,T.A. (1989) *Science*, **246**, 1135–1142.
2. Rould,M.A., Perona,J.J. and Steitz,T.A. (1991) *Nature*, **352**, 213–218.
3. Ruff,M., Krishnaswamy,S., Boeglin,M., Poterszman,A., Mitschler,A., Podjarny,A., Rees,B., Thierry,J.C. and Moras,D. (1991) *Science*, **252**, 1682–1689.
4. Giegé,R., Puglisi,J.D. and Florentz,C. (1992) *Progr. Nucleic Acids Res. Mol. Biol.*, in press.
5. Pütz,J., Puglisi,J.D., Florentz,C. and Giegé,R. (1991) *Science*, **252**, 1696–1699.
6. Rudinger,J., Puglisi,J.D., Pütz,J., Schatz,D., Eckstein,F., Florentz,C. and Giegé,R. (1992) *Proc. Natl. Acad. Sci. U. S. A.*, **89**, 5882–5886.
7. Moras,D., Comarmond,M.B., Fischer,J., Weiss,R., Thierry,J.C., Ebel,J.P. and Giegé,R. (1980) *Nature*, **288**, 669–674.
8. Westhof,E., Dumas,P. and Moras,D. (1985) *J. Mol. Biol.*, **184**, 119–145.
9. Sampson,J.R., DiRenzo,A.B., Behlen,L.S. and Uhlenbeck,O.C. (1990) *Biochemistry*, **29**, 2523–2532.
10. Perret,V., Florentz,C., Puglisi,J.D. and Giegé,R. (1992) *J. Mol. Biol.*, **226**, 323–333.
11. Francklyn,C. and Schimmel,P. (1989) *Nature*, **337**, 478–481.
12. Lorber,B., Kern,D., Dietrich,A., Gangloff,J., Ebel,J. and Giegé,R. (1983) *Biochem. Biophys. Res. Com.*, **117**, 259–267.
13. Wyatt,J.R., Chastain,M. and Puglisi,J.D. (1991) *BioTechniques*, **11**, 764–769.
14. Perret,V., Garcia,A., Puglisi,J., Grosjean,H., Ebel,J.P., Florentz,C. and Giegé,R. (1990) *Biochimie*, **72**, 735–744.
15. Perret,V., Garcia,A., Grosjean,H., Ebel,J.P., Florentz,C. and Giegé,R. (1990) *Nature*, **344**, 787–789.
16. Vlassov,V.V., Giegé,R. and Ebel,J.P. (1981) *Eur. J. Biochem.*, **119**, 51–59.
17. Romby,P., Moras,D., Dumas,P., Ebel,J.P. and Giegé,R. (1987) *J. Mol. Biol.*, **195**, 193–204.
18. Puglisi,J.D. and Tinoco,I.Jr (1989) *Methods in Enzymology*, **180**, 304–325.
19. Ehresmann,C., Baudin,F., Mougel,M., Romby,P., Ebel,J.P. and Ehresmann,B. (1987) *Nucleic Acids Res.*, **15**, 9109–9128.
20. Tuerk,C., Gauss,P., Thermes,C., Groebe,D.R., Gayle,M., Guild,N., Stormo,G., d'Aubenton-Carafa,Y., Uhlenbeck,O.C., Tinoco,I.Jr, Brody,E.N. and Gold,L. (1988) *Proc. Natl. Acad. Sci. U.S.A.*, **85**, 1364–1368.
21. Coutts,S.M., Gangloff,J. and Dirheimer,G. (1974) *Biochemistry*, **13**, 3938–3948.
22. Romby,P. (1986) *Thèse d'Etat*, University of Strasbourg, France.
23. Crothers,D.M., Cole,P.E., Hilbers,C.W. and Schulman,R.G. (1974) *J. Mol. Biol.*, **87**, 63–88.
24. Woese,C.R., Winker,S. and Gutell,R.R. (1990) *Proc. Natl. Acad. Sci. U. S. A.*, **87**, 8467–8471.
25. Westhof,E., Dumas,P. and Moras,D. (1988) *Acta Cryst.*, **A44**, 112–123.
26. Varani,G., Cheong,C. and Tinoco,I.Jr. (1991) *Biochemistry*, **30**, 3280–3289.
27. Holbrook,S.R., Sussman,J.L., Warrant,W.R., Church,G.M. and Kim,S.-H. (1977) *Nucleic Acids Res.*, **8**, 2811–2820.
28. Jack,A., Ladner,J.E., Rhodes,D., Brown,R.S. and Klug,A. (1977) *J. Mol. Biol.*, **111**, 315–328.
29. Westhof,E., Dumas,P. and Moras,D. (1988) *Biochimie*, **70**, 140–165.
30. Stein,A. and Crothers,D.M. (1976) *Biochemistry*, **15**, 160–168.
31. de Bruijn,M.H.L. and Klug,A. (1983) *EMBO J.*, **2**, 1309–1321.
32. Okimoto,R. and Wolstenholme,D.R. (1990) *EMBO J.*, **9**, 3405–3411.
33. Kumazawa,Y., Yokogawa,T., Hasegawa,E., Miura,K. and Watanabe,K. (1989) *J. Biol. Chem.*, **264**, 13005–13011.
34. Mans,R.M.W., Pleij,C.W.A. and Bosch,L. (1991) *Eur. J. Biochem.*, **201**, 303–324.
35. Romby,P., Moine,H., Lesage,P., Graffe,M., Dondon,J., Ebel,J.P., Grunberg-Manago,M., Ehresmann,B., Ehresmann,C. and Springer,M. (1990) *Biochimie*, **72**, 485–494.
36. Mohr,G. and Lambowitz,A.M. (1991) *Nature*, **354**, 164–167.
37. Puglisi,J.D., Tan,R., Calnan,B.J., Frankel,A.D. and Williamson,J.R. (1992) *Science*, **257**, 76–80.